Proc. Natl. Acad. Sci. USA
Vol. 89, pp. 6162–6166, July 1992
Cell Biology

Changes in intracellular calcium during the development of epithelial polarity and junctions

(tight junction/Madin–Darby canine kidney cell/fura-2)

SANJAY K. NIGAM*, ENRIQUE RODRIGUEZ-BOULAN†‡, AND RANDI B. SILVER‡

*Department of Medicine, Harvard Medical School, Brigham and Women's Hospital and the Harvard Center for the Study of Kidney Diseases, Boston, MA 02115; and ‡Departments of Physiology and Anatomy and Cell Biology, Cornell University Medical College, New York, NY 10021

Communicated by Bernard L. Horecker, March 19, 1992

ABSTRACT **The "Ca^{2+} switch" model with cultured Madin–Darby canine kidney (MDCK) cells is useful in studying the biogenesis of epithelial polarity and junction formation and provides insight into early steps in the morphogenesis of polarized epithelial tissues. When extracellular Ca^{2+} in the medium is changed from <5 μM to 1.8 mM, MDCK cells rapidly change from a nonpolarized state exhibiting little cell–cell contact (with the apical membrane and junctional proteins largely within the cell) to a polarized state with well-formed tight junctions and desmosomes. To examine the role of intracellular Ca^{2+} in the development of polarity and junctions, we made continuous spectrofluorimetric measurements of intracellular Ca^{2+} during the "switch," using the fluorescent indicator fura-2. Intracellular Ca^{2+} increased >10-fold during the switch and gave a complex pattern of increase, decrease, and stabilization. In contrast, intracellular pH [monitored with 2',7'-bis(2-carboxyethyl)-5(and 6)-carboxyfluorescein (BCECF)] did not change during the period studied. When intracellular Ca^{2+} curves in several cells were compared, considerable heterogeneity in the rate of increase of intracellular Ca^{2+} levels and in peak levels was evident, perhaps reflecting the heterogeneity among cells in establishing junctions and polarity. The heterogeneity of the process was confirmed by digital imaging of intracellular Ca^{2+} and was present even in a "clonal" line of MDCK cells, indicating the heterogeneity was intrinsic to the process and not simply a function of slight genetic variation within the population of MDCK cells. In pairs of cells that had barely established cell–cell contact, often one cell exhibited a much greater increase in intracellular Ca^{2+} than the other cell in the pair. At the site of cell–cell contact, an apparent localized change (an increase over the basal level) in intracellular Ca^{2+} was frequently present and occasionally appeared to extend beyond the point of cell–cell contact. Since the region of cell–cell contact is also the site where junctions form and where vesicles containing apical membranes fuse during the development of polarity, we postulate a role for global and local changes in intracellular Ca^{2+} in these events.**

Signaling events involved in the development of epithelial cell–cell contact, tight and desmosomal junctions, and apical–basolateral polarity remain poorly defined. In the case of the establishment of cell–cell contact and tight junctions, extracellular Ca^{2+} is thought to play an important role, as removal of Ca^{2+} from the exterior of the cell (the medium) prevents cell adhesion (1) and results in the disruption of tight junctions in established monolayers (2). Furthermore, in a Madin–Darby canine kidney (MDCK) cell model for tight-junction formation, the "Ca^{2+} switch" model, raising the extracellular Ca^{2+} in the medium from <5 μM to 1.8 mM causes confluent MDCK cells exhibiting little cell–cell contact and virtually no tight-junction formation to establish cell–cell contact and to develop tight junctions within hours, as determined by transepithelial resistance and the immunofluorescent localization of the tight-junctional protein ZO1 (3–6). Moreover, the Ca^{2+} switch model, which is thought to mimic processes occurring during the morphogenesis of epithelial tissues (compaction), is also an excellent model for the development of epithelial polarity. Under conditions of low Ca^{2+} concentrations, the MDCK cells exhibit incomplete development of apical–basolateral polarity (4). In fact, much of the apical membrane appears within a recently described organelle [the vacuolar apical compartment (VAC)] that contains microvillar structures and thus will stain not only for apical proteins but also for actin (5). Increasing Ca^{2+} in the medium triggers the rapid fusion of VAC with the plasma membrane at a site believed to be in close proximity to the site of initial cell–cell contact and tight-junction assembly (5).

While it is clear that Ca^{2+} plays a role in cell–cell contact and tight-junction formation on the extracellular side (1, 2), the role of intracellular Ca^{2+} in the processes leading to cell–cell contact, the sorting of tight-junctional and desmosomal components, and the development of apical–basolateral polarity remains to be defined. Cuvette measurements of intracellular Ca^{2+} with different fluorescent dyes (indo-1 and quin-2) in the Ca^{2+} switch model have yielded conflicting results (4, 7). To explore the role of intracellular Ca^{2+} in the development of cell–cell contact, tight junctions, and epithelial polarity in the Ca^{2+} switch model, we have studied changes in intracellular Ca^{2+} during the "switch," using a combination of spectrofluorimetric and digital imaging techniques. The results indicate complex temporal and spatial changes in intracellular Ca^{2+} during the switch that may be related to the development of junctions and polarity.

METHODS

Materials. Nigericin in 3:1 (vol/vol) ethanol/dimethyl sulfoxide and acetoxymethyl (AM) esters of fura 2 and BCECF [2',7'-bis(2-carboxyethyl)-5(and 6)-carboxyfluorescein] (both made up in dimethyl sulfoxide) were from Molecular Probes.

Ca^{2+} Switch. MDCK cells (≈passage 30) grown to confluence were incubated in phosphate-buffered saline (PBS) for 20 min, followed by treatment with trypsin in EDTA until a virtual single-cell suspension resulted. The cells were allowed to attach for ≈75 min to rat tail collagen (type I)-coated coverslips (≈2.5 × 105 cells per cm^2) in Dulbecco's modified Eagle's medium (DMEM) containing 5% (vol/vol) fetal calf

The publication costs of this article were defrayed in part by page charge payment. This article must therefore be hereby marked "*advertisement*" in accordance with 18 U.S.C. §1734 solely to indicate this fact.

Abbreviations: MDCK cells, Madin–Darby canine kidney cells; VAC, vacuolar apical compartment; LC and NC media, low-calcium and normal-calcium media; BCECF, 2',7'-bis(2-carboxyethyl)-5(and 6)-carboxyfluorescein.

†To whom reprint requests should be addressed at: Department of Anatomy and Cell Biology, Cornell University Medical College, 1300 York Avenue, New York, NY 10021.

serum (FCS); the DMEM formulation includes 1.8 mM Ca^{2+} [normal Ca^{2+} (NC) medium]. The coverslips were then carefully washed six times in minimal essential medium (MEM) modified for suspension cultures (SMEM), which lacks $CaCl_2$ and contains <5 μM Ca^{2+}, as previously confirmed by Ca^{2+} electrode (6) [low-Ca^{2+} (LC) medium]. This was followed by an ≈16-hr incubation in SMEM containing 5% FCS that had been dialyzed extensively against PBS and EGTA as described (1). For immunofluorescence studies, "switch" experiments were initiated by quickly replacing the SMEM with DMEM containing 5% FCS (NC medium).

Immunofluorescent Analysis. Immediately prior to the Ca^{2+} switch and 50 min after the Ca^{2+} switch was begun, MDCK cells growing on coverslips were fixed in PBS containing 2% paraformaldehyde for 20 min at room temperature or were fixed for ZO1 staining in −80°C methanol and incubated at −20°C for 20 min. The cells were then washed three times with PBS and subjected to permeabilization with PBS containing 0.075% saponin (PBS-S) for 5 min. The permeabilized cells were then incubated for ≈60 min with either a rat monoclonal antiserum in PBS-S against the tight-junctional marker ZO1 (1:100, gift of D. Goodenough, Harvard) or [after blocking for 1 hr in PBS containing 2% (wt/vol) bovine serum albumin] a polyclonal antiserum against the apical marker glycoprotein gp135 (1:500, gift of G. Ojakian, SUNY, Health Science Center at Brooklyn) and fluorescein isothiocyanate-conjugated phalloidin (1:200, Sigma). The cells were then washed three times with PBS-S, followed by incubation with rhodamine-conjugated second antibody in PBS-S for ≈45 min, which was then followed by five washes of 3 min each in PBS-S.

Single-Cell Measurements of Intracellular Ca^{2+} and pH. Cells grown on Corning 18-mm coverslips were placed "cell side up" in a flow-through Lucite chamber fitted on the top with a standard glass coverslip. Cells were loaded by incubation in 5 μM fura-2 or 10 μM BCECF in medium. Media (LC medium without phenol red and vitamins or NC medium without phenol red and vitamins) were gravity fed into an experimental chamber mounted on the stage of an inverted epifluorescence microscope (Zeiss IM35) equipped with quartz interior components. The flow rate through the chamber averaged 2.3 ml/min. The microscope was interfaced to an alternating wavelength illumination system (Delta SCAN, Photon Technology International [PTI]), which provides light at two alternating wavelengths and is equipped with a 75-W Xenon lamp. Individual cells are excited at 340 nm and 380 nm with emission at 510 nm for intracellular Ca^{2+} measurements and at 440 nm and 490 nm with emission at 520 nm for intracellular pH measurements. An individual cell was aligned in the viewfinder leading into the photomultiplier tube. The output of the photometer was stored in a computer that also controlled the illumination system. Before each experiment, autofluorescence was measured on a single cell on an unloaded coverslip, and this value was automatically subtracted from subsequent traces.

For Ca^{2+} measurements, individual coverslips were incubated with 5 μM fura-2 for 30 min at room temperature. The coverslip was then attached to the chamber and superfused with LC solution for at least 10 min prior to the start of measurements. Calibration was carried out at the end of each experiment on a single cell with the Ca^{2+} ionophore ionomycin (10 μM) in the presence of NC medium (maximum ratio) or 2 mM EGTA in LC medium (minimum ratio). Ca^{2+} levels were calculated as described by Grynkiewicz *et al.* (8). In the case of pH measurements with BCECF, calibration was performed at the end of each experiment on each cell studied. Extracellular pH was varied from 6.8 to 7.8 in potassium Ringer's solution (145 mM) in the presence of 10 μM nigericin by the method of Thomas *et al.* (9).

Digital Imaging. Digital imaging of intracellular Ca^{2+} was performed under conditions identical to the single-cell measurements already described. A PTI dual monochromator (340 nm/380 nm) imaging system with a Hamamatsu SIT C2400 camera was used. Cells were viewed through a Nikon diaphot microscope with a ×40 Nikon fluorite oil-immersion objective.

RESULTS

MDCK cells plated at confluence and maintained overnight (≈16 hr) under conditions with low (<5 μM) Ca^{2+} concentration were generally round and exhibited little cell–cell contact (Fig. 1 *Right*). By indirect immunofluorescence, the tight-junctional protein ZO1 was found either inside the cell (Fig. 1*A*) or localized to discrete zones on or underneath the surface of the cell, indicating that even in low Ca^{2+} concentrations (which is thought to synchronize the process), the tight junctions in this model system are in various stages of formation. Immunofluorescence using antisera against the apical marker protein gp135 (Fig. 1*B*) and detection of actin (with fluorescein isothiocyanate-conjugated phalloidin; Fig. 1*C*), which together are markers for the VAC, revealed the presence of intracellular vesicles in ≈20% of the cells characteristic of VAC staining. Again, the heterogeneity of the process should be noted, since a number of cells did not

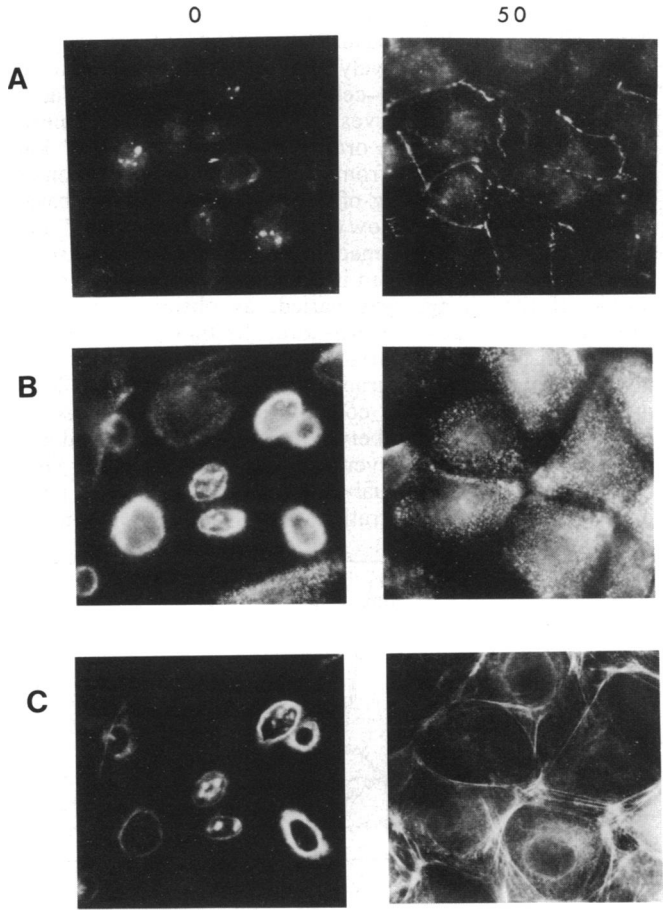

FIG. 1. Cytochemical localization of tight-junctional protein ZO1 (*A*), apical membrane protein gp135 (*B*), and actin (*C*) immediately prior to (0 min) (*Left*) and 50 min after (*Right*) the Ca^{2+} switch. MDCK cells were attached to coverslips, incubated for 16 hr in SMEM and "switched" as described in text. ZO1 and gp135 were detected with monospecific antisera, and actin was detected with fluorescein isothiocyanate-conjugated phalloidin. *B* and *C* represent double staining of the same field of cells. (×≈640)

possess clearly discernible VACs and appeared to be further on in the pathway toward apical membrane formation.

Within 50 min after the Ca^{2+} level in the medium was switched to 1.8 mM, contact between cells was well established, and the staining characteristic of tight junctions was apparent on the lateral surfaces (Fig. 1*A* at 50 min). This is consistent with the observation that "switched" MDCK cells develop a significant transepithelial electrical resistance shortly after this time (3, 6). Also by 50 min, the apical membrane marker protein gp135 had largely moved from intracellular sites to the cell surface, thus forming the apical membrane (Fig. 1*B*), and actin filament staining was found primarily in the submembranous cytoskeleton. Although at 50 min the classical fluorescent patterns of tight junctions, apical membrane, and subcortical actin filaments were clearly beginning to be established, at intermediate time points the heterogeneity of the processes was quite evident, with different cells in various stages of junction and apical-membrane formation (data not shown).

To address the role of intracellular Ca^{2+} in these processes, we performed continuous single-cell spectrofluorimetric measurements of cytosolic Ca^{2+} with the fluorescent indicator fura-2 before and during the Ca^{2+} switch. Earlier cuvette measurements represent means of the intracellular Ca^{2+} changes occurring in the whole population in the cuvette and do not provide insight into changes occurring at the individual cell level or cellular regions. To address this apparent contradiction, we performed fura-2 studies at the single-cell level with a photomultiplier tube and then applied ratio imaging to fura-2-loaded cells. Relatively round cells that appeared to be beginning to establish cell–cell contact were selected. Fig. 2 shows five individual curves representing separate experiments on single cells. The ordinate is the apparent Ca^{2+} ion concentration calculated from the intracellular calibration of the dye. At the beginning of the trace, the apparent basal intracellular Ca^{2+} level is low (10 nM). Upon "switching" the extracellular Ca^{2+} in the medium to 1.8 mM (at ≈150 sec), intracellular Ca^{2+} increased in all cases; however, the magnitude of the change was varied, as observed in these representative traces. Furthermore, the time course of the change was also quite variable, with some cells exhibiting very rapid increases in intracellular Ca^{2+} and others following a much slower time course. The rate of increase in intracellular Ca^{2+} varied between 18 nM Ca^{2+}/min and 478 nM Ca^{2+}/min, with an average rate of 134 nM Ca^{2+}/min (Table 1). In 10 individual cells studied, the mean peak intracellular Ca^{2+} concentration was 326 (± 96) nM, which is more than a 30-fold increase over the basal level (Table 1). In addition, by about 15 min, the intracellular Ca^{2+} tended to stabilize at a Ca^{2+} level that was ≈1 order of magnitude greater than the preswitch Ca^{2+} (10 nM vs. 109 nM), which was still somewhat higher than that measured in MDCK cells grown to confluence in NC medium (60 ± 12 nM, n = 21). In marked contrast, single-cell measurements of intracellular pH using the fluorescent dye BCECF showed no change in pH during the period of the switch monitored (Fig. 3). Thus, this single-cell data not only indicated a marked change in intracellular Ca^{2+} levels during the switch (without a concomitant change in pH) but also revealed the process to be highly heterogeneous.

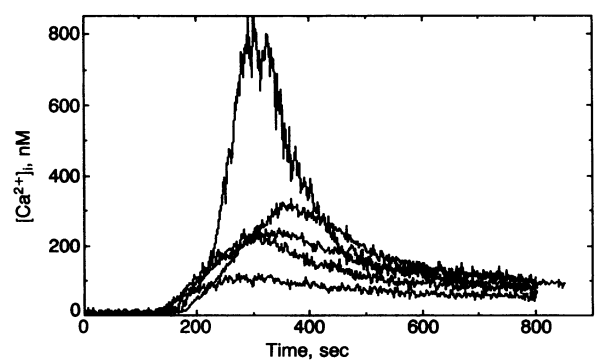

FIG. 2. Single-cell spectrofluorimetric measurements of intracellular Ca^{2+} concentration ($[Ca^{2+}]_i$) in fura-2-loaded cells during the switch. The five curves represent five individual cells during five different switches performed on the same day. The ordinate corresponds to $[Ca^{2+}]_i$ based on the intracellular calibration of fura-2 in each cell. The switch occurred at ≈150 sec. These representative traces reflect the varied responses observed in terms of the magnitude of change and rate of increase in $[Ca^{2+}]_i$ as a result of the switch.

This marked heterogeneity was further documented by using digital imaging, where we monitored the response of all of the cells in the field during the switch. Fig. 4 is a four-paneled pseudocolor representation of a field of relatively round cells exhibiting various degrees of cell–cell contact. The bar scale at the right of Fig. 4 depicts a pseudocolor key to 340 nM/380 nM ratios obtained from fura-2 fluorescence and is thus a direct indication of intracellular Ca^{2+} levels. Fig. 4 *Upper Left* was taken at time 0 with the cells bathed in LC medium. The switch was performed at ≈200 sec, and other panels were taken after the switch.

Consistent with the single-cell measurements, under conditions of low Ca^{2+} concentrations, the intracellular Ca^{2+} was extremely low (Fig. 4 *Upper Left*). At various time points after the switch, intracellular Ca^{2+} increased in all cells (isolated cells included) but with great heterogeneity in both the rate and degree of increase, as was expected from the curves obtained from single-cell measurements. That this heterogeneity in intracellular Ca^{2+} increase, decrease, and stabilization was not due to genetic heterogeneity among the type II MDCK cells being studied was excluded when the same experiment was performed with an early-passage clonal line of MDCK cells selected from the same population of type II MDCK cells used for all of the other experiments. During the switch, the clonally selected line (clone E16, courtesy of Ivan R. Nabi, Cornell University Medical College) showed a heterogeneous response similar to that of the unselected type II MDCK cells (not shown).

In pairs of cells that had established contact with one another, frequently one cell exhibited a much greater increase in intracellular Ca^{2+} than the cell with which it had established contact (Fig. 4). In addition, at the site of cell–cell contact, there was an apparent localized change in intracellular Ca^{2+} (note the yellow area between abutting cells; see white arrowheads). In the field shown, this occurred in all three pairs of round cells that had established contact. It was also seen in the round cell (upper right corner of each panel) abutting the more flattened diamond-shaped cells. Moreover, the same phenomenon was observed in one of the diamond-shaped cells (follow the starred cell in *Upper Left*) abutting another diamond-shaped cell. In this cell, the localized

Table 1. Intracellular Ca^{2+} measurements (Ca_i^{2+}) in single MDCK cells superfused with LC solution and then switched to NC solution

Ca_i^{2+}, nM			
LC	NC peak	NC steady state	ΔCa_i^{2+}/min
10.20 ± 2.64	325.5 ± 96.1	108.5 ± 20.2	134.0 ± 52.0

Analysis of the data obtained from spectrofluorometric measurements of intracellular Ca^{2+} concentration ($[Ca^{2+}]_i$) in 10 MDCK cells switched from LC to NC solution. The $[Ca^{2+}]_i$ values in NC represent the peak of the response and the steady-state value at 10 min after the switch. The change in $[Ca^{2+}]_i$ per min reflects the initial rate of increase of $[Ca^{2+}]_i$ during the switch. Values are means ± SEM (n = 10).

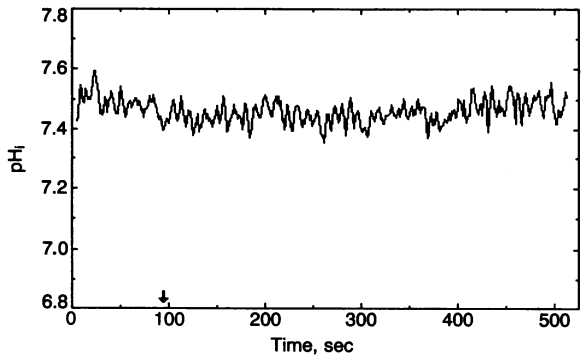

FIG. 3. Representative trace of continuous single-cell spectrofluorimetric measurements of intracellular pH (pH_i) in a BCECF-loaded cell during the switch. The ordinate represents the corresponding pH_i associated with the intracellular calibration of the dye in this cell. The switch from superfusing the cell with LC solution to NC solution occurred at the arrow. In four other similar experiments, pH_i did not change significantly during the period monitored.

change in Ca^{2+} extended well beyond the site of cell–cell contact, occurring along two sides of the diamond-shaped (starred) cell. This latter finding addresses a potential problem with the digital-imaging evidence that suggests a localized change in intracellular Ca^{2+} at sites of cell–cell contact. In the three pairs of cells already described, it is difficult to exclude the possibility that the localized change in Ca^{2+} level at sites of cell–cell contact is due to an optical scattering effect from two juxtaposed cells with different fura-2 ratios. The fact that in the diamond-shaped (starred) cell, the localized change extends well beyond the region of cell–cell contact suggests that the localized change observed is not an optical effect. Furthermore, in other digital images of "switched" cells, the apparent localized change was seen even when the difference in ratios between two abutting cells was not nearly as great as in those pairs shown in Fig. 4. In a few cases, frequent successive images suggested that the region of localized change can develop before the intracellular Ca^{2+} in the cell with the higher Ca^{2+} reaches its peak.

DISCUSSION

With spectrofluorimetric measurements of intracellular Ca^{2+} (Fig. 2 and Table 1), we have established that there is a marked increase in intracellular Ca^{2+} during the Ca^{2+} switch, in agreement with cuvette measurements obtained in an earlier study (7). Moreover, in contrast with the earlier studies, we have been able to follow the rapid changes in intracellular Ca^{2+} during the switch by continuously measuring "ratioed" fura-2 fluorescence in single cells. In addition to establishing a complex pattern of increase, decrease, and stabilization of intracellular Ca^{2+}, these measurements have revealed the process to be highly heterogeneous when single cells were compared. This may reflect the heterogeneity of cells during the Ca^{2+} switch in the development of junctions and the formation of the apical membrane [as a result of fusion of the VAC (Fig. 1)].

The marked and complex changes in intracellular Ca^{2+} during the switch, the heterogeneity of the response, and the possibility that localized changes in intracellular Ca^{2+} might also be important led us to characterize Ca^{2+} changes in a select field of cells by using ratioed digital images during the switch (Fig. 4). The digital images confirmed the single-cell measurements and provided additional evidence for the heterogeneity of the process. In pairs of abutting cells, often one cell exhibited a much greater increase in intracellular Ca^{2+} than the other cell in the pair. The mechanism and significance of this observation are unclear, but its frequency is striking. However, this may indicate "recruitment" by the cell with higher Ca^{2+} of the other cell in the pair, possibly by liver cell adhesion molecule-mediated (L-CAM) signaling or movement of the ion through gap junctions or Ca^{2+} channels at the site of cell–cell contact.

The digital images also suggested that localized changes in intracellular Ca^{2+} may occur at the site of cell–cell contact during the switch. As already discussed, we are aware of the possibility that the apparent localized rise could conceivably be an optical effect due to the juxtaposition of two cells with different Ca^{2+} levels. However, the fact that images were obtained where the localized change extended well beyond the site of cell–cell contact suggests that the localized change is not due to optical scattering created by two different ratios in abutting cells. The regulation of intracellular Ca^{2+} is very complex (10); the mechanism of this apparent localized change in Ca^{2+} (involvement of local Ca^{2+} channels, inositol trisphosphate-sensitive and -insensitive intracellular stores, gap junctions between cells, or some combination of these) remains to be elucidated.

The lack of significant change in intracellular pH during the period monitored was somewhat surprising in view of the fact that confluent MDCK cells incubated in LC medium had previously been reported to exhibit a decline in intracellular pH (11), possibly (as has been hypothesized) caused by an effect of the Na^+/Ca^{2+}-exchanger on the Na^+/H^+-antiporter (12). Moreover, because the rapid decline in Ca^{2+} (over a period of seconds) after the intracellular Ca^{2+} level peaks during the switch might be due to uptake into stores by an intracellular Ca^{2+}-ATPase [which has been postulated to be coupled to proton transport in the opposite direction (13)], changes in intracellular pH might also be expected. Although we did not observe a change in intracellular pH, given the array of mechanisms regulating intracellular pH and the variety of intracellular buffering mechanisms, it is important not to overinterpret this result.

The intracellular Ca^{2+} measurements and the imaging data raise a number of other questions that will require further examination. The specific role of intracellular Ca^{2+} in tight-junction formation and VAC fusion is as yet unclear. Since extracellular Ca^{2+} appears necessary for establishing cell–cell contact and junction formation (1, 2), it has been difficult to unambiguously separate the role of extracellular Ca^{2+} in these processes from the role of intracellular Ca^{2+}. It seems likely that both extracellular and intracellular Ca^{2+} are important in the formation and maintenance of intercellular junctions. Perhaps cell–cell contact not only requires Ca^{2+} in the medium but also results in an increase in intracellular Ca^{2+} either by direct entry into the cells or by release from intracellular stores. It should be emphasized that both tight-junction formation and VAC fusion are believed to occur at sites of cell–cell contact (possibly mediated by liver cell adhesion molecule [L-CAM] and/or other cell surface molecules) (5, 14), raising the intriguing possibility that the apparent localized changes in intracellular Ca^{2+} during the switch may play a role in the fusion of nascent tight-junctional vesicles and VAC with the plasma membrane. Such a role does not seem unlikely in view of evidence from other systems suggesting a role for intracellular Ca^{2+} in many terminal secretory events (15, 16). Nevertheless, these fusion events probably occur within minutes after the switch (Fig. 1 and ref. 4), long before the development of transepithelial electrical resistance, and it is difficult to directly assess by current methods the role of Ca^{2+} in the fusion of VAC and nascent tight-junctional vesicles. It is also worth noting that, during the switch, assembly of other junctions (desmosomes, gap, adherens) and marked changes in cell shape and volume occur (17, 18). Whether intracellular Ca^{2+} plays a role in these processes, possibly through remodeling of the cytoskeleton during the switch, needs to be determined.

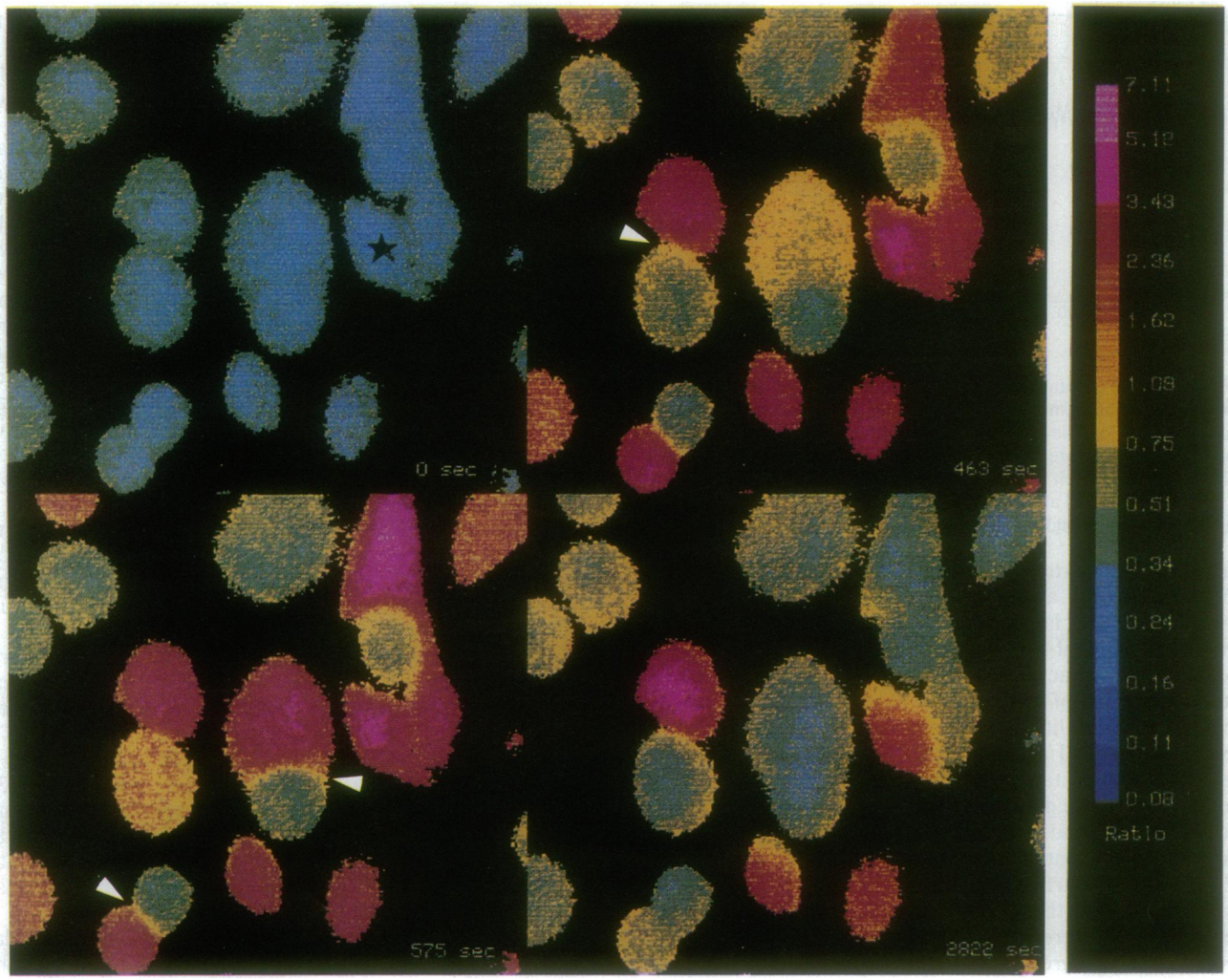

FIG. 4. Digital imaging of intracellular Ca^{2+} in fura-2-loaded MDCK cells during the switch. Details are provided in text. A pseudocolor key to the ratioed images is shown at the right (red-white = high ratio = high Ca_i, blue = low ratio = low Ca_i). The switch was performed at approximately 200 sec. Similar images were obtained in a clonal population of MDCK cells. Several regions of apparent localized changes in intracellular Ca^{2+} at sites of cell–cell contact are indicated by white arrowheads. See text for discussion of the starred cell.

Ca^{2+} is necessary for the activation of a number of intracellular enzymes involved in signal transduction, including protein kinase C. We have shown (6) that tight-junction formation in the Ca^{2+} switch model is inhibited by the protein kinase inhibitor H7. Perhaps localized increases in intracellular Ca^{2+} result in protein kinase C activation, which then modulates the formation of tight junctions. Since the Ca^{2+} switch model is believed to mimic events during the development of epithelial tissues, it seems plausible that a similar course of events may be important in, for example, the process of compaction during kidney tubulogenesis (14, 19).

We thank Karoly Csatorday (Photon Technology, New Brunswick, NJ) and Kevin Strange (Harvard Medical School and Children's Hospital, Boston) for invaluable help in obtaining and analyzing the digital images. S.K.N. thanks Barry M. Brenner for suggesting the Ca^{2+} switch as a model in which the connections between the cellular-signaling and protein-sorting systems might be studied. R.B.S. is the recipient of an Andrew T. Mellon Teacher/Scientist Award. E.R.-B. is a recipient of National Institutes of Health Grant GM-34107 and a New York Heart Association Grant-in-Aid.

1. Gumbiner, B. & Simons, K. (1986) *J. Cell Biol.* **102,** 457–468.
2. Martinez-Palamo, A., Meza, I., Beaty, G. & Cerejido, M. (1980) *J. Cell Biol.* **87,** 736–745.
3. Gonzalez-Mariscal, L., Chavez de Ramirez, B. & Cerejido, M. (1985) *J. Membr. Biol.* **86,** 113–125.
4. Vega-Salas, D., Salas, P. J. & Rodriguez-Boulan, E. (1987) *J. Cell Biol.* **104,** 1249–1259.
5. Vega-Salas, D., Salas, P. J., & Rodriguez-Boulan, E. (1988) *J. Cell Biol.* **107,** 1717–1728.
6. Nigam, S. K., Denisenko, N., Rodriguez-Boulan, E. & Citi, S. (1991) *Biochem. Biophys. Res. Commun.*, **181** 548–553.
7. Gonzales-Mariscal, L., Contreras, R. G., Bolivar, J. J., Ponce, A., Chavez de Ramirez, B. & Cereijido, M. (1990) *Am. J. Physiol.* **259,** C978–C986.
8. Grynkiewicz, G., Poenie, M. & Tsien, R. Y. (1985) *J. Biol. Chem.* **260,** 3440–3450.
9. Thomas, J. A., Buchsbaum, R. N., Zimniak, A. & Racker, E. (1979) *Biochemistry* **18,** 2210–2218.
10. Lytton, J. & Nigam, S. K. (1992) *Curr. Opin. Cell Biol.* **4,** 220–226.
11. Borle, A. B., Borle, C. J., Dobransky, P., Gorecka-Tisera, A. M., Bender, C. & Swain, K. (1990) *Am. J. Physiol.* **259,** C19–C25.
12. Borle, A. B. & Bender, C. (1991) *Am. J. Physiol.* **261,** C482–C489.
13. Schulz, I., Thevenod, F. & Dehlinger-Kremer, M. (1989) *Cell Calcium* **10,** 325–326.
14. Rodriguez-Boulan, E. & Nelson, W. J. (1989) *Science* **245,** 718–725.
15. Sarafian, T., Pradel, L., Henry, J., Aunis, D. & Bader, M. (1991) *J. Cell Biol.* **114,** 1135–1147.
16. Burgoyne, R. D. (1990) *Annu. Rev. Physiol.* **52,** 647–659.
17. Pasdar, M. & Nelson, W. J. (1989) *J. Cell Biol.* **109,** 163–177.
18. Nelson, W. J. & Veshnock, P. (1987) *J. Cell Biol.* **104,** 1527–1537.
19. Brenner, B. M. (1990) *J. Am. Soc. Nephrol.* **1,** 127–139.